

Temperature Control in (Translucent) Phase Change Materials Applied in Facades A Numerical Study

Tenpierik, Martin; Wattez, Yvonne; Turrin, Michela; Cosmatu, Tudor; Tsafou, Stavroula

10.3390/en12173286

Publication date

Document Version Final published version

Published in **Energies**

Citation (APA)Tenpierik, M., Wattez, Y., Turrin, M., Cosmatu, T., & Tsafou, S. (2019). Temperature Control in (Translucent) Phase Change Materials Applied in Facades: A Numerical Study. *Energies*, *12*(17), Article 3286. https://doi.org/10.3390/en12173286

Important note

To cite this publication, please use the final published version (if applicable). Please check the document version above.

Other than for strictly personal use, it is not permitted to download, forward or distribute the text or part of it, without the consent of the author(s) and/or copyright holder(s), unless the work is under an open content license such as Creative Commons.

Takedown policy

Please contact us and provide details if you believe this document breaches copyrights. We will remove access to the work immediately and investigate your claim.





Article

Temperature Control in (Translucent) Phase Change Materials Applied in Facades: A Numerical Study

Martin Tenpierik *, Yvonne Wattez, Michela Turrin, Tudor Cosmatu and Stavroula Tsafou

Department of Architectural Engineering + Technology, Faculty of Architecture and the Built Environment, Delft University of Technology, 2628 BL Delft, The Netherlands

* Correspondence: m.j.tenpierik@tudelft.nl

Received: 7 August 2019; Accepted: 24 August 2019; Published: 26 August 2019

Abstract: Phase change materials (PCMs) are materials that can store large amounts of heat during their phase transition from solid to liquid without a significant increase in temperature. While going from liquid to solid this heat is again released. As such, these materials can play an important role in future energy-efficient buildings. If applied in facades as part of a thermal buffer strategy, e.g., capturing and temporarily storing solar energy in so-called Trombe walls, the PCMs are exposed to high solar radiation intensities, which may easily lead to issues of overheating. This paper therefore investigates the melting process of PCM and arrives at potential solutions for countering this overheating phenomenon. This study uses the simulation program Comsol to investigate the heat transfer through, melting of and fluid flow inside a block of PCM (3 × 20 cm²) with a melting temperature of around 25 °C. The density, specific heat and dynamic viscosity of the PCM are modeled as a temperature dependent variable. The latent heat of the PCM is modeled as part of the specific heat. One side of the block of PCM is exposed to a heat flux of 300 W/m². The simulations show that once part of the PCM has melted convection arises transporting heat from the bottom of the block to its top. As a result, the top heats up faster than the bottom speeding up the melting process there. Furthermore, in high columns of PCM a large temperature gradient may arise due to this phenomenon. Segmenting a large volume of PCM into smaller volumes in height limits this convection thereby reducing the temperature gradient along the height of the block. Moreover, using PCMs with different melting temperature along the height of a block of PCM allows for controlling the speed with which a certain part of the PCM block starts melting. Segmenting the block of PCM using PCMs with different melting temperature along its height was found to give the most promising results for minimizing this overheating effect. Selecting the optimal phase change temperatures however is critical in that case.

Keywords: phase change materials; facades; heat transfer; computational fluid dynamics; convection

1. Introduction

In order to mitigate climate change and move towards a society based on renewable energy sources, the primary (fossil) energy consumption of societies needs to be significantly reduced. Buildings are responsible for a large share of this primary energy consumption, which in the European Union is in the order of 40% [1]. Space heating and space cooling are the dominant contributors to this building-related energy consumption. Particularly improving the energy performance of facades, making them part of a smart and bioclimatic design, will be a key enabler. Novel materials, like phase change materials, may play a pivotal role in such future high performance buildings.

Energies **2019**, 12, 3286 2 of 16

Phase change materials are materials that can store large quantities of heat in the transition from solid to liquid without significant change in temperature. When they cycle from liquid to solid this heat will again be released. Phase change materials (PCMs) come in different types. Paraffins are interesting because of their large latent heat of fusion, low cost and good chemical stability but are highly flammable and non-transparent, this latter property being highly interesting for applications in facades of buildings. For buildings, particularly the salt-hydrates and bio-based PCMs are interesting among others because they are non-flammable or not easily flammable. Furthermore, the salt-hydrates are relatively cheap, have a large latent heat of fusion and can be transparent in liquid state. These PCMs are however corrosive and have limited chemical stability. Bio-based PCMs are based on materials like palm oil and soy oil, can be transparent in liquid state, have good chemical stability, limited flammability and are non-corrosive. A disadvantage of these PCMs is their low density, which means that more volume is needed in order to reach the same heat storage capacity as compared to many other PCMs; and they are generally more expensive [2].

Several review papers explain the potential of the use of PCMs in buildings, e.g., for interior application, for application as part of HVAC (Heating, Ventilation and Air-Conditioning) systems or for application in facades [3–7]. Over the past decade, research efforts have increasingly focused on the application of (transparent) PCMs in facades. For instance, Gutherz and Schiler [8], Weinläder et al. [9], Soares et al. [10], Fiorito [11], Goia et al. [12,13], Turrin et al. [14], Wang and Zhao [15], Wattez et al. [16] and Tenpierik et al. [17] investigated the use of phase change materials to capture heat from the sun, temporarily store this heat and finally release it into a room with a time delay of several hours. Furthermore, Weinläder et al. [18], Komerska et al. [19] and Li et al. [20] looked into the use of PCMs as a sun protection system. In all these applications the PCMs might be exposed to high solar radiation intensities, which may easily lead to issues of overheating if the facade system is not designed properly. These studies so far, however, did only look at the general behavior of the PCM based on heat transfer simulations only; they did not look into how the PCM itself behaves on a material level like non-parallel melting fronts, fluid flow, overheating, etc.

Only a few studies exist that study the actual melting behavior of PCM considering the different behavior of the liquid and solid phase, albeit generally not focusing on application in buildings or facades of buildings. As shown by among others Jegadheeswaran and Pohekar [21], Murray and Groulx [22], Bertrand et al. [23], Tay et al. [24] and Wang and Zhao [15], if a block of PCM is exposed to a heat source, fluid flow arises in the liquid phase of the PCM, which generally transports heat from the bottom of the PCM to its top. This redistribution of heat causes the temperature to rise faster at the top of the PCM. This speeds up the melting process there and increases the temperature gradient from the bottom to the top. Furthermore, in case of high solar radiation intensities this may easily lead to PCM overheating at the top of the block. This paper will therefore further investigate the melting process of PCM applied in facades and exposed to a strong heat source like solar radiation. As such it will advance the work conducted by Murray and Groulx [22] and Ogoh and Groulx [25]. This study is unique because it arrives at potential solutions for countering PCM overheating for applications with a strong heat source. The results of such studies are essential for proper application of PCMs in facades of buildings.

This research is part of the Double Face 2.0 research project in which a lightweight, translucent, adjustable Trombe wall is being investigated [14,16,17]. This Trombe wall consists of a layer of PCM with a melting temperature of around 25 °C and a thin (1 cm) layer of translucent aerogel grains. During a winter's day the layer of PCM is facing the window where it is exposed to solar radiation (Figure 1). The heat from the sun is then captured and stored inside the PCM. The thin layer of aerogel ensures that the heat is being trapped and does not immediately start heating up the space behind the wall. In the evening the Trombe wall rotates so that the PCM layer is facing the room where it can slowly give off its heat into the space. As such the Trombe wall acts as a heating device bridging the time difference between the presence of solar radiation and the need for heat when people are at home. This paper lays the foundations for follow-up papers that will focus on the optimization of the Trombe wall surface and inner structure from a heat transfer and fluid flow perspective.

Energies **2019**, 12, 3286 3 of 16

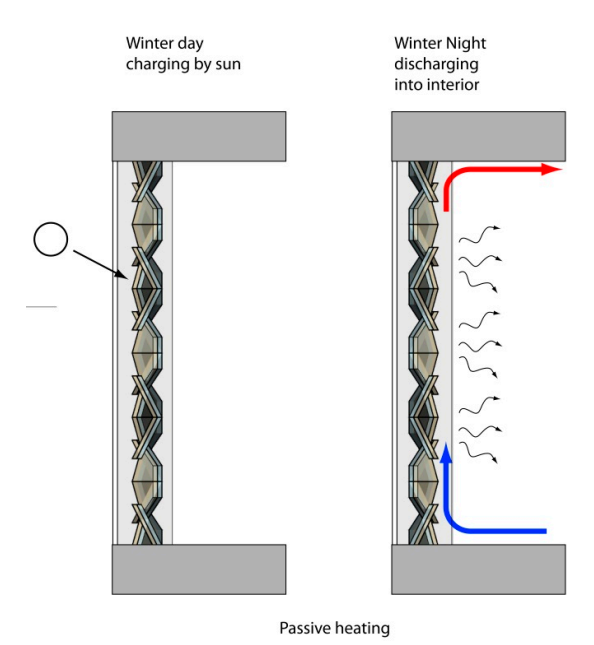


Figure 1. Double Face 2.0 Trombe wall winter operation mode [17].

2. Materials and Methods

In this paper the results of measurements and simulations will be described using a phase change material with a phase change near 25 °C. Below, first the properties of the phase change material will be described. Next, the methodology of the measurements will be explained followed by the methodology of the simulations with.

2.1. Phase Change Material

In the measurements and simulations a PCM with a phase change centered around 25 °C during the melting process was taken. This melting temperature was selected based on studies performed by Fiorito [11] and Castellon et al. [26]. In the simulations, hysteresis was ignored. The density of the PCM was 1500 kg/m³ in the solid state and 1400 kg/m³ in the liquid state (modeled as continuous second derivative smoothing with an absolute size transition zone of 4 °C centered around 25 °C). From 27 °C and up it follows a similar change in density as seen in water. The density was therefore modeled as a temperature dependent variable with a density as shown in Figure 2. The latent heat of the PCM was 180 kJ/kg within a temperature range from 17 °C to 32 °C. The sensible specific heat equaled 2 kJ/kg/K. The latent heat was modeled as part of the specific heat, c_P , by raising this value from 2 kJ/kg/K to a value that was specified by the manufacturer (Figure 3). Besides, similarly to Murray and Groulx [22] the PCM was modeled as a liquid with a temperature dependent dynamic viscosity. The viscosity was chosen high (1·10⁴ Pa·s) for the solid state as a result of which the modeled liquid behaved as a solid in that state. The liquid state of the PCM had a dynamic viscosity of 1·10⁻² Pa·s (Figure 4) as a result of which it behaved as a liquid in that state (modeled as continuous second derivative smoothing with an absolute size transition zone of 4 °C). Comsol version 5.3 also has the option of directly modeling a phase change material by providing the properties of the solid and the liquid state separately. In this research that option was not selected in order to have better control over the behavior of the PCM during the phase change. The thermal conductivity of the material was constant at 0.6 W/m/K. The opacity of the PCM on the solar spectral band and ambient spectral band were both set to transparent in the simulations.

In some simulations (step 3) PCMs with a melting temperature of 23 °C, 24 °C, 27 °C and 29 °C were used as well. For these materials the same properties were used as for the PCM with a melting temperature 25 °C. However, the curves from Figures 2 to 4 were shifted with -1 °C, -2 °C, +2 °C or +4 °C respectively.

Energies 2019, 12, 3286 4 of 16

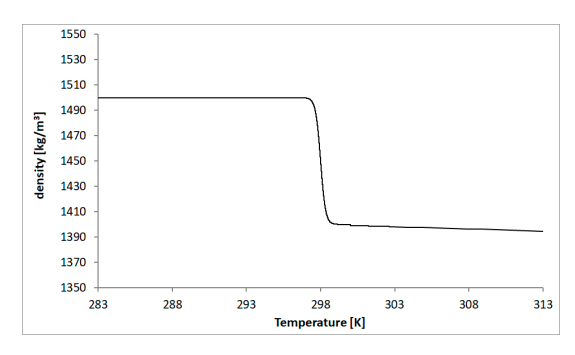


Figure 2. Density of used phase change materials (PCM).

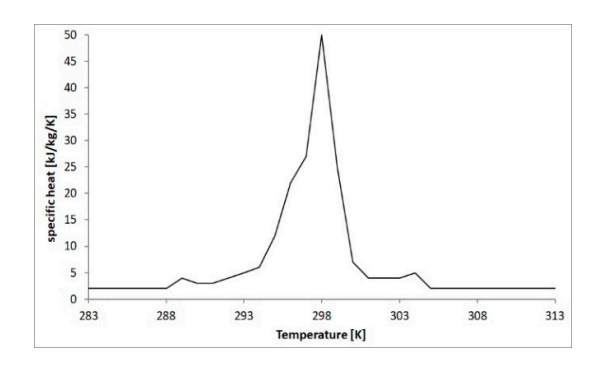


Figure 3. Specific heat of used PCM.

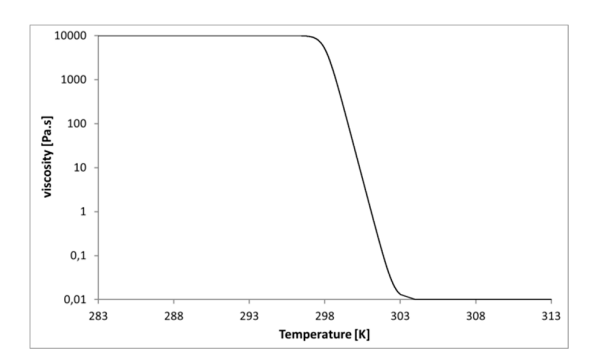


Figure 4. Dynamic viscosity of used PCM.

2.2. Measurements for Model Validation

The model and material properties were validated by comparing a Comsol model to physical measurements in a test box. The test box was a cubic box of 1 m³ air surrounded by 12 cm Styrofoam. The box was heated to a temperature of around 45 °C using an incandescent light bulb shielded by a thin layer of aluminum foil in order to make sure it was not radiating heat onto the test sample. One side of the box contained a hole of 14×14 cm² in which the test sample was placed. As a result, the test sample was exposed to a temperature of around 45 °C on one side and to room temperature (around 21.5 °C) on the other side.

The test sample was a container made of PMMA (Poly(methyl methacrylate)) with an outer dimension of 14 × 14 cm² and a thickness of 4.2 cm. The inner volume of 12 × 12 × 3 cm³ was filled with PCM with a melting temperature around 25 °C, the properties of which were explained in Section 2.1. For the simulation PMMA was selected from the materials library in Comsol v5.3a with the accompanying built-in properties.

The temperature inside the box, on both surfaces of the test sample and of the room were measured with a type T thermocouple connected to an Eltek GENII GS24 transmitter. The heat fluxes into/out of both surfaces of the sample were measured with two Hukseflux HFP01 heat flux plates

Energies **2019**, 12, 3286 5 of 16

connected to an Eltek GENII GS44 transmitter. The transmitters transmitted their data wirelessly to an Eltek RX250-AL data logger, which could be read out via a computer with Darca Plus software. The measurements and simulation were run for a time of 24 hours.

Concerning the simulation in Comsol, the settings as explained in Sections 2.1 and 2.4.2 were used. Exceptions were the initial condition for the temperature, which was 21.5 °C matching the initial temperature of the experiment. Furthermore, the boundary conditions were different. The side of the sample facing the inside of the box had two convective heat flux boundaries: One with a heat transfer coefficient of 6.0 W/(m²-K) representing radiative heat transfer at the respective temperatures; one with a heat transfer coefficient calculated by Comsol using the 'external forced convection' option (with a height of 0.14 m and an air speed of 0.5 m/s due to a small fan active inside the test box). The first value representing radiative heat transfer, the second convective heat transfer. The side of the sample facing the room also had two convective heat flux boundaries: One with a heat transfer coefficient of 5.2 W/(m²-K) for radiation heat transfer and a calculated heat transfer coefficient for natural convection. This latter value was calculated by Comsol by setting it to 'external natural convection' along a 'vertical wall' with height 0.14 m. This heat transfer coefficient ranged between 0 and 4 W/(m²-K) throughout the simulations. The results of the measurements will be presented in Section 3.1.

2.3. Simulation Model Test

In order to test the simulation model to ensure that all settings in Comsol were correct, the results from Murray and Groulx [22] were precisely replicated. The exact same settings and material properties as presented in their paper were used for this test, except for the value of the dynamic viscosity for which 0.08 Pa·s instead of 0.008 Pa·s was used in order to get practically the same results. Based on numerous tests with varying settings in Comsol (all combinations of the values of the variables from the paper were tested to check the results), it is almost certain that Figure 5 in their paper is based on a dynamic viscosity of 0.08 Pa·s. Furthermore, the viscosity profile of Figure 4 in their paper was used instead of the formula that is written in their text (the figure and the formula do not entirely correspond). They simulated a block of 0.1 × 0.1 cm² of octadecane with Comsol version 4.0a and 4.1, which was exposed to a constant temperature of 303 K on one side of the block and a temperature of 313 K on the other side. The top and bottom of the block were given an insulation boundary and the initial temperature was set to 303 K. They present their results after a simulated time of 5000 s. The results of our replication simulation (also after 5000 s) are presented in Figure 5. This figure shows practically the same outcome as presented by Murray and Groulx [22] in their Figure 5. In general, these results show that the right settings and material properties were included in our model in Comsol. It is interesting to mention that Murray and Groulx [22] also compare their results to those of Bertrand et al. [23] who did calculations of the position of the melting front according to different models found in the literature. They concluded that their simulated results showed the same shape of the melting front as found by Bertrand et al. [23]. However, slightly less melting was observed. We now assume based on this comparison that the modeling of the melting process in Comsol was done properly.

The models used in our paper in which we modeled the melting process of a salt hydrate PCM involved a few differences as compared to the model of Murray and Groulx [22], which partly are due to new functionalities in Comsol version 5.3a:

- Gravity was modeled not as a separate volume force but as the built-in option of included gravity. Furthermore, the density was specified not as a constant but as a temperature dependent variable as shown in Figure 2.
- The density, specific heat and dynamic viscosity functions of the PCM were all modeled with continuous second derivative smoothing.
- Furthermore, the boundary conditions were different. In our model, we exposed the PCM block
 to a heat flux of 300 W/m² instead of an imposed temperature of 313 K. The mesh and time
 stepping was also set specifically for these new simulations. The boundary on which the

Energies **2019**, 12, 3286 6 of 16

radiation flux was set was opaque for the radiation while the PCM itself was transparent on spectral band in liquid state.

 The walls exposed to radiation or an imposed temperature had a no slip condition instead of a slip condition better matching the results from our physical measurements (see Section 3.1).

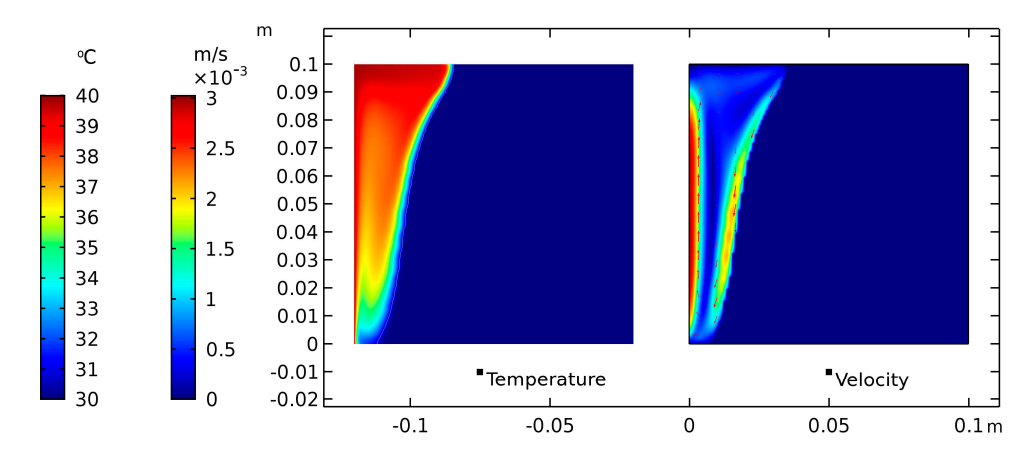


Figure 5. Results of the replication simulation of the model by Murray and Groulx [21] after t = 5000 s.

2.4. Simulation Methodology

2.4.1. Overall Simulation Methodology

This study used a 2D numerical approach using Comsol version 5.3a as the simulation engine. Conduction, convection and radiation were included as modes of heat transfer and also fluid flow was considered. The following physics interfaces were included in this study: Heat transfer in fluids and creeping flow. Creeping flow was selected because after some initial tests the results showed that the flow of the molten PCM had a low speed (order of 0.5 mm/s) and as a result a low Reynolds number.

This study first explored the melting process of a single block of PCM (10 × 10 cm²) specifically focusing on the shape of the melting front. This first simulation was also meant to validate the model by comparing it to the results obtained by Bertrand et al. [23] and Murray and Groulx [22]. Next, a block of PCM of 3 cm thick and 20 cm high was investigated as one block, as a segmented block with five blocks of each 4 cm high, and as a segmented block with 10 blocks of each 2 cm high. In the final third step the segmented block of PCM (five segments) was modeled with five different PCMs with different melting temperatures: 23 °C, 24 °C, 25 °C, 27 °C and 29 °C. The PCM blocks were stacked on top of each other starting with the lowest melting temperature at the bottom and then with increasing melting temperature towards the top. Figure 6 gives a graphical representation of this process.

Energies **2019**, 12, 3286 7 of 16

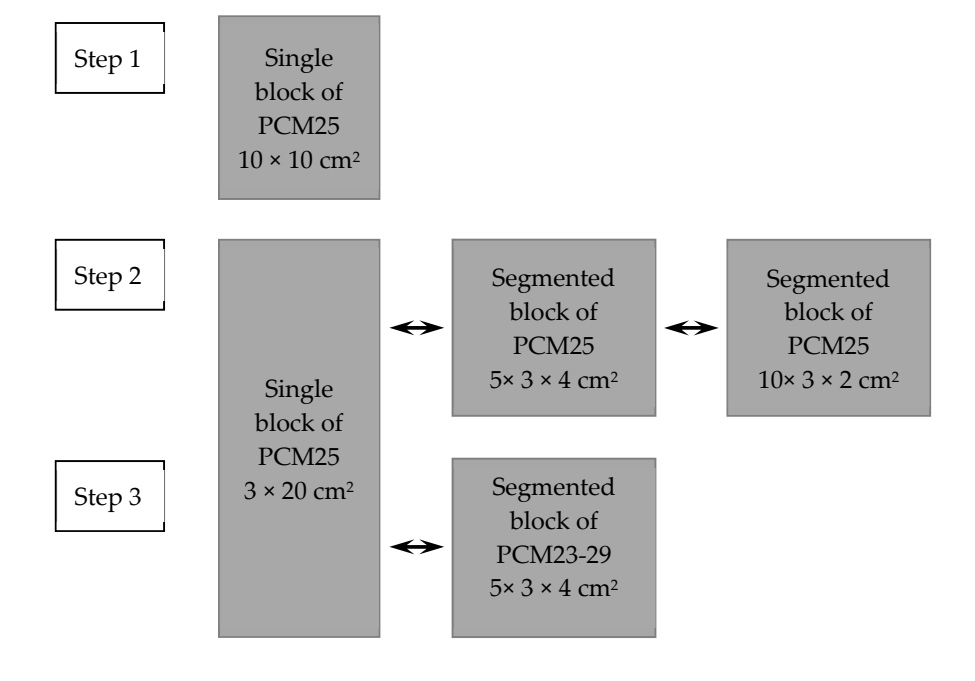


Figure 6. Research overview.

2.4.2. Simulation Settings and Boundary Conditions

For the creeping flow physics interface the settings from Table 1 were used. The settings for the heat transfer in the fluids physics interface are presented in Table 2. These settings represent realistic settings that were validated by comparing simulations to measurements (see Sections 2.2 and 3.1). The boundary conditions on the PCM block are shown in Figure 7. A heat flux of 300 W/m² was selected representing an average (over the heating season months of Jan.-Apr. and Oct.-Dec.) of the average high heat flux on a south facing facade of a building throughout the entire day for the city of Amsterdam in the Netherlands; according to the EnergyPlus epw weather file for Amsterdam this value is approximately 306 W/m². We selected the average high and not the normal average because in this paper we were investigating solutions for overcoming overheating of PCM. A convective heat transfer boundary with a heat transfer coefficient (h) of 10 W/m²/K and a constant temperature of 20 °C were modeled on the other side of the block. This condition represents indoor conditions and the heat transfer coefficient represents a combination of IR radiation exchange plus convective heat transfer exchange with slightly raised temperature of the object. In case of the stacked blocks of PCM, the different blocks were separated by an internal wall with no slip conditions. This internal wall (without material properties) allowed for heat transfer to take place along this boundary but did not allow for continuous fluid flow.

Table 1. Settings for creeping flow interface.

Property	Setting/Value
Ambient temperature	293.15 K
Ambient abs. pressure	1 atm.
Ambient rel. humidity	0
Wind velocity	0 m/s
Initial values	T = 293.15 K

Table 2. Settings for heat transfer in fluids interface.

Property Setting/Value			
Compressibility	Compressible flow (Ma < 0.3)		
Turbulence model	None		

Energies **2019**, 12, 3286 8 of 16

Gravity	Included				
Reference pressure level	1 atm.				
Reference temperature	293.15 K				
Deference resition	x = 0 m				
Reference position	y = 0 m				
	$u_{\rm x} = 0 {\rm m/s}$				
Initial values	$u_{\rm y} = 0 \mathrm{m/s}$				
	p = 0 Pa				
Compensate for hydrostatic pressure approximation					
Wall conditions	No slip				
Inner wall conditions	If they exist: No slip				
Neglect internal term (Stokes flow)					

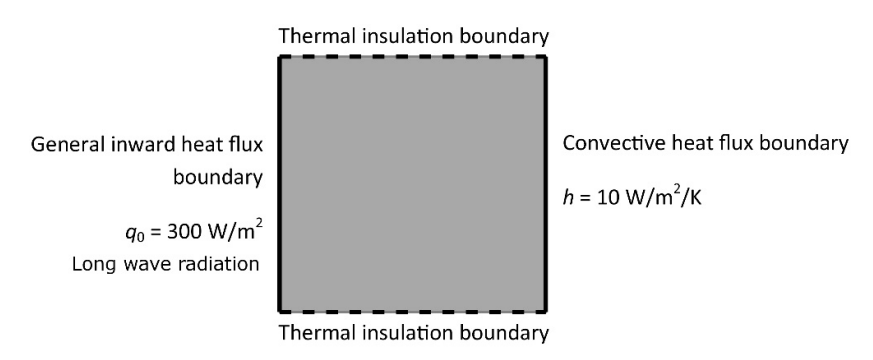


Figure 7. Thermal boundary conditions on the modeled PCM block.

2.4.3. Mesh Sizing and Solver Settings

A simulation was run for 16 hours with a time step per minute. Relative tolerance was set to 0.001 and the Paradiso solver was used for the simulations. For defining the mesh, the general mesh was set as user-defined with a predefined 'extra fine' element size calibrated for fluid dynamics. A free quad mesh type was used. A one boundary layer was included with a stretching factor of 1.2 and automatic thickness of the first layer. For the first block of PCM (step 1) this led to 6237 domain elements and 308 boundary elements. Simulation runtime was about 53 minutes on a quad Intel® $core^{TM}$ i7-8650U CPU @1.90 GHz/2.11 GHz processor. For the second unsegmented block of PCM (step 2 unsegmented) this led to 40,681 domain elements and 1180 boundary elements with a simulation runtime of approximately 82 minutes. For the second segmented block (five segments of $3 \times 4 \text{ cm}^2$) to 21,188 domain elements and 1338 boundary elements with an approximated runtime of 19 minutes for step 2 and 56 minutes for step 3. For the second segmented block (10 segments of $3 \times 2 \text{ cm}^2$) to 20,760 domain elements and 1538 boundary elements with an approximated runtime of around 178 minutes.

3. Results and Discussion

3.1. Results of the Measurements (PMMA Container Willed with $12 \times 12 \times 3$ cm³ of PCM)

Figure 8a,b show the comparison of the temperatures respectively heat fluxes between the physical measurements and the simulations in Comsol. The lines denote the results from the simulation while the circles and crosses represent the results from the measurements. As can be seen, the simulation model in general predicted the temperatures and surface heat transfer relatively well. Some differences emerged due to inaccuracies in selected heat transfer coefficients and in inaccuracies in the properties of the PCM (the manufacturer states up to 7.5% deviation in latent heat storage capacity). The root mean square deviation (RMSD) of the temperature on the hot side and cold side equaled 0.7 °C and 1.2 °C, respectively; and the root mean square deviation of the heat flux on the hot and cold side equaled 13.9 W/m² and 6.7 W/m² respectively. Based on these results we therefore assumed that our simulation model was good enough to be used for further investigations. The results of these further investigations will be presented in the next sections.

Energies **2019**, 12, 3286 9 of 16

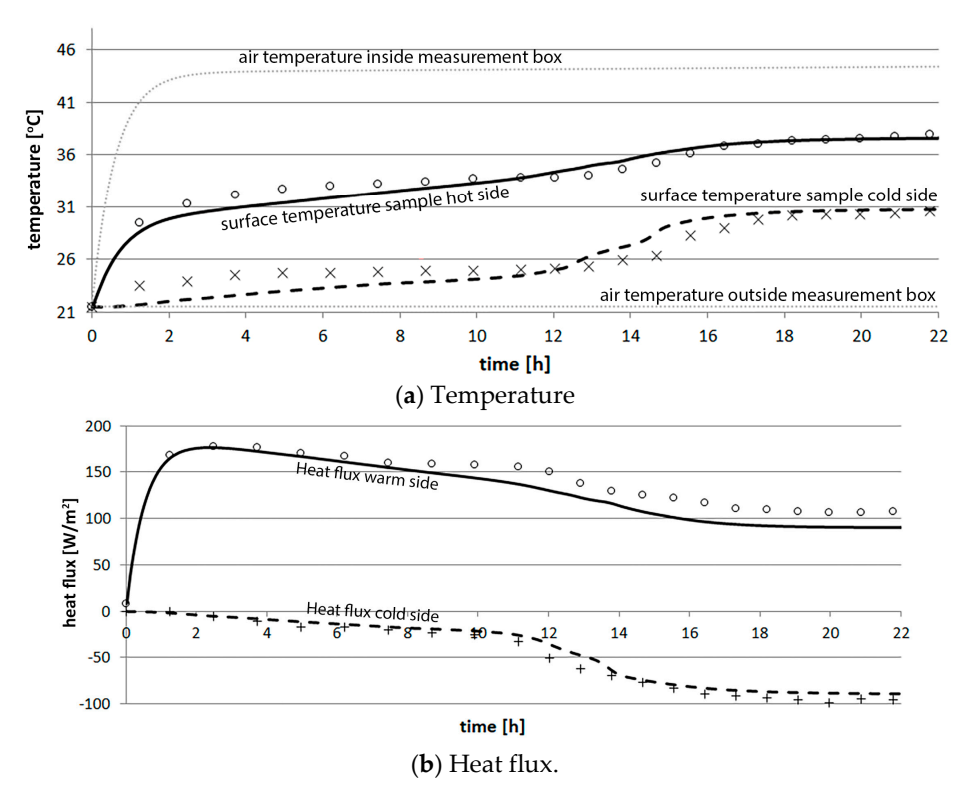


Figure 8. Results of the validation of the simulation model by physical measurements.

3.2. Simulation Step 1 (Single Block of PCM25 10 × 10 cm²)

Figure 9 shows the results of the simulations of the single block of PCM25 of 10 × 10 cm². The white lines in the temperature contour plot denote the 23 °C and 27 °C isotherms denoting the boundaries between which phase change occurred while the black line shows the 25 °C isotherm. As can be seen, even though the heat flux onto the surface was uniform along this surface, the heating process was not similarly uniform (1D). Only in the early phases of the heating process, when the PCM was still completely in the solid phase, the PCM slowly heated up from one side in a manner parallel to this surface (isotherms parallel to the exposed surface). However, once the first amounts of PCM had molten, which was already after around 2 hours, fluid flow would transport heat from the bottom of the block towards the top, speeding up the heating process at the top. As such the isotherms started to bend near the top of the block of PCM. This behavior is in line with what was reported by Bertrand et al. [23] and Murray and Groulx [22]. However, differences arose because of the use of a different type of PCM with different properties and different boundary conditions (imposed temperature on one side of the PCM block versus imposed heat flux on the PCM block).

3.3. Simulation Step 2 (Single and Segmented Blocks of PCM25 3 × 20 cm²)

Three simulations were run using just a block of PCM (either in full height 20 cm \times 3 cm, in height segmented in five blocks of 3×4 cm² or in height segmented in ten blocks of 3×2 cm²) exposed to a radiation source of 300 W/m² for 16 h from one side. Figures 10–12 present the results of these simulations. As can be seen, segmenting the full block of PCM in height into smaller blocks led to a more uniform heating of the PCM and as a result in a smaller temperature gradient from bottom to top after 8 hours of melting. The temperature at the top of the PCM stack was lower whereas the temperature at the bottom was a bit higher in the segmented case than in the unsegmented case, both after 8 hours (Table 3). After 16 hours (Table 4) the temperature difference between the top and bottom of the stack was more or less identical for all simulated case, around 16 °C. This shows that

Energies 2019, 12, 3286 10 of 16

the lower part of the PCM more quickly melts if the PCM block is segmented. For applications of PCM in facades the 8 hour exposure time was more relevant than the 16 hour exposure time.

In each of the PCM segments after a while convection cells start to emerge that transport heat from the bottom of a segment to its top. Furthermore, some of that heat was transported via conduction from the top of one segment to the bottom of the segment on top as a result of which the segment at the top of the entire stack still heated up faster than the lower segments. However, the smaller the segments, the less pronounced this effect is.

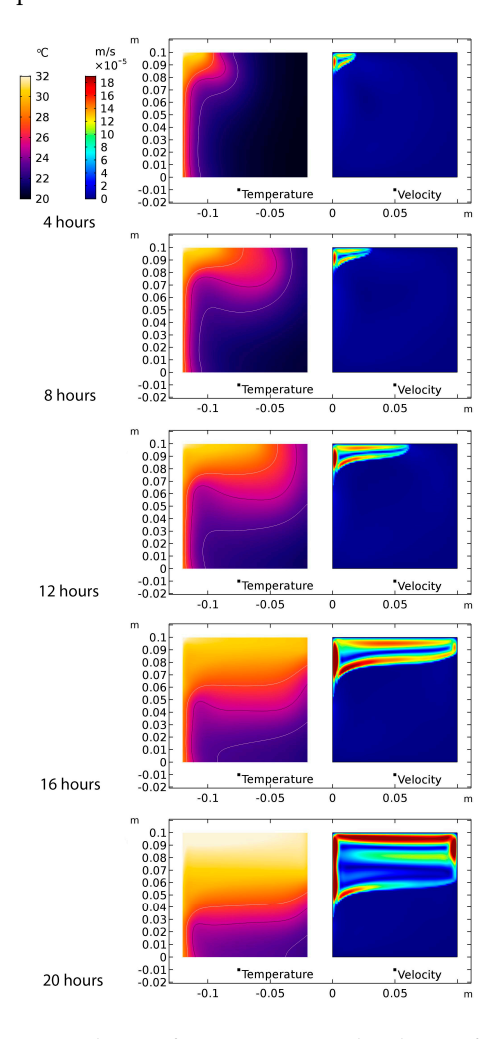


Figure 9. Results of the step 1 simulation after 4, 8, 12, 16 and 20 hours (from top to bottom); black line in temperature contour plot is the 25 °C isotherm; white lines are the 23 °C respectively 27 °C isotherms.

Table 3. Minimum (bottom), maximum (top) and average temperatures of the PCM after 8 hours.

Cham	Sample	Tmin	T_{max}	$T_{\text{max}} - T_{\text{min}}$	Tav
Step		(°C)	(°C)	(°C)	(°C)
2	single block of PCM25 3 × 20 cm ²	23.0	48.4	25.4	36.0
2	segmented block of PCM25 5 × 3 × 4 cm ²	24.0	43.9	19.9	33.9
2	segmented block of PCM25 10 × 3 × 2 cm ²	24.6	43.1	18.5	34.3
3	segmented block of PCM23-29 5 × 3 × 4 cm ²	26.5	39.3	12.8	32.9

Table 4. Minimum (bottom), maximum (top) and average temperatures of the PCM after 16 hours.

	Step	Sample	Tmin	Tmax	$T_{\text{max}} - T_{\text{min}}$	Tav
--	------	--------	------	------	-----------------------------------	-----

Energies 2019, 12, 3286 11 of 16

		(°C)	(°C)	(°C)	(°C)
2	single block of PCM25 3 × 20 cm ²	42.6	58.5	15.9	50.2
2	segmented block of PCM25 5 × 3 × 4 cm ²	42.9	59.0	16.1	50.6
2	segmented block of PCM25 10 × 3 × 2 cm ²	43.2	59.3	16.1	50.9
3	segmented block of PCM23-29 5 × 3 × 4 cm ²	43.1	59.1	16.0	50.7

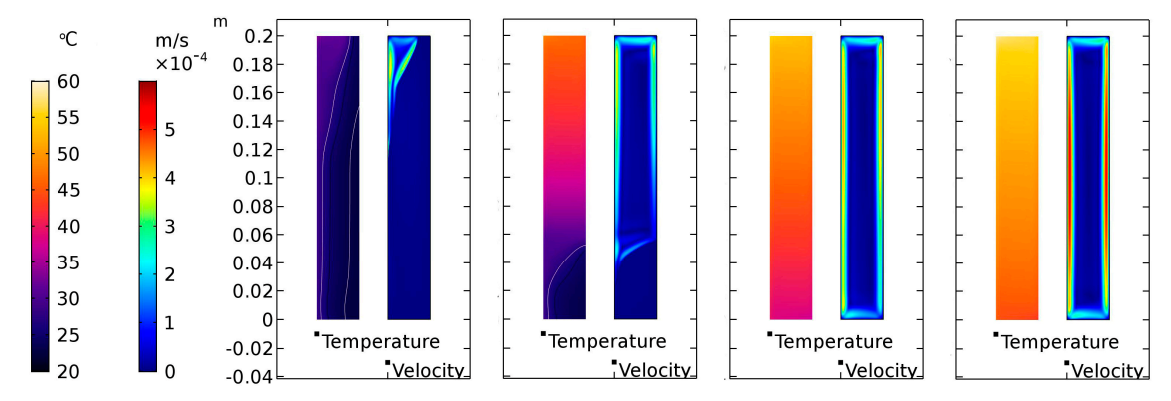


Figure 10. Results of the step 2 simulation for the unsegmented block after 4, 8, 12 and 16 hours (from left to right); black line in temperature contour plot is the 25 $^{\circ}$ C isotherm; white lines are the 23 $^{\circ}$ C respectively 27 $^{\circ}$ C isotherms.

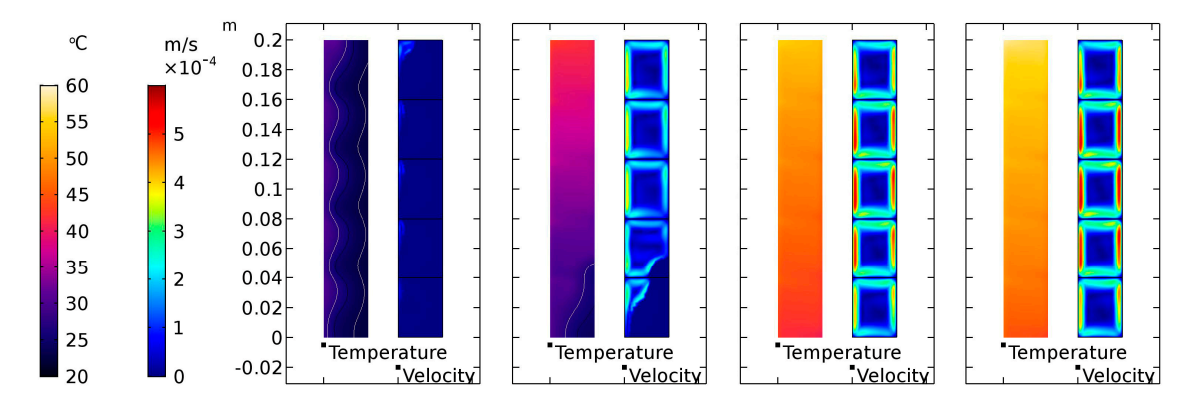


Figure 11. Results of the step 2 simulation for the segmented block (5 segments of 3×4 cm²) after 4, 8, 12 and 16 hours (from left to right); black line in temperature contour plot is the 25 °C isotherm; white lines are the 23 °C respectively 27 °C isotherms.

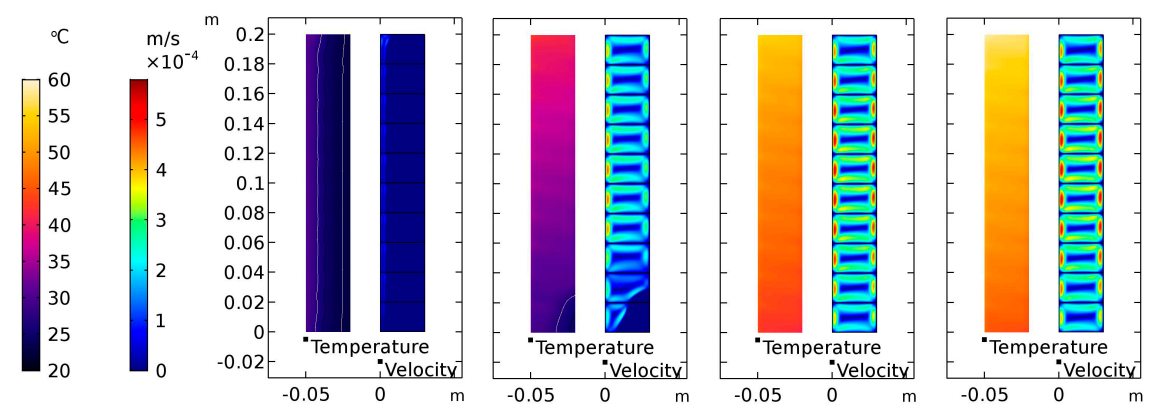


Figure 12. Results of the step 2 simulation for the segmented block (10 segments of 3×2 cm²) after 4, 8, 12 and 16 hours (from left to right); black line in temperature contour plot is the 25 °C isotherm; white lines are the 23 °C respectively 27 °C isotherms.

Energies **2019**, 12, 3286 12 of 16

3.4. Simulation Step 3 (Segmented Block of PCM23-29 3 × 20 cm²)

As a final step a simulation was run with the segmented block with five segments but with different PCM melting temperatures: 23 °C/24 °C/25 °C/27 °C/29 °C from bottom to top. The PCM blocks were stacked on top of each other starting with the lowest melting temperature at the bottom and then with increasing melting temperature towards the top. The results of the simulations are shown in Figure 13. As seen, using PCMs with different melting temperatures stacked on top of each other also allowed for better controlling the melting process throughout the entire column of PCM. By using a lower melting temperature at the bottom, the lower segments of PCM will melt quicker; by using a higher melting temperature at the top, the higher segments of PCM will start melting later.

Looking at the temperature gradient from bottom to top that emerged in the PCM stack, this gradient only was smaller than the gradient for the same configuration but with PCM25 after 8 hours (Table 3) but not after 16 hours (Table 4). After 16 hours of melting all simulated variants led to a similar temperature difference between the top and bottom of around 16 °C. For applications in facades, this therefore was a good choice—considering that an 8 hour exposure time was more relevant, especially under winter conditions in a temperate climate. The precise exposure time will depend on the location of the building, the orientation of the facade and the time of year. However, optimizing the PCM melting temperatures in such a stack for the right application may make this option interesting because it allows control over the melting process throughout the entire stack (Figure 13 after 8 hours).

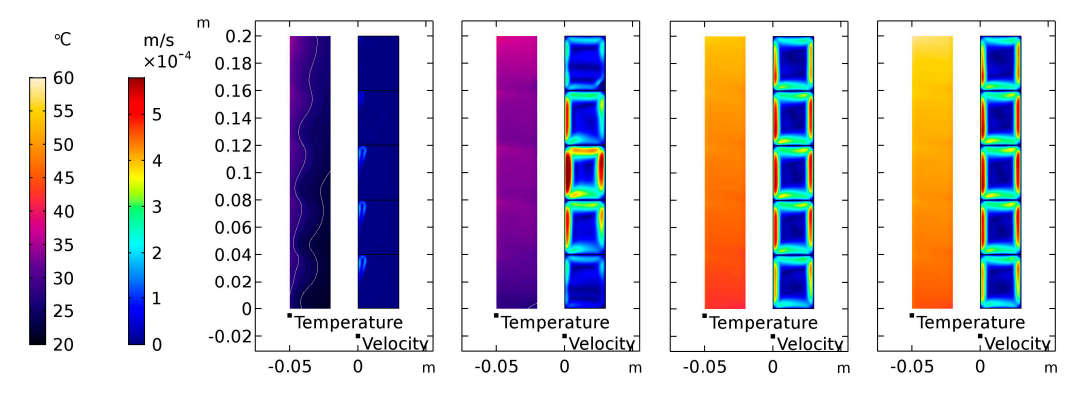


Figure 13. Results of the step 3 simulation for the segmented block (5 segments of 3×4 cm²) with different PCM melting temperatures after 4, 8, 12 and 16 hours (from left to right); black line in temperature contour plot is the 25 °C isotherm; white lines are the 23 °C respectively 27 °C isotherms. PCMs have melting temperatures of around 23 °C, 24 °C, 25 °C, 27 °C and 29 °C from bottom to top.

3.5. Comparison of the Average PCM Temperatures

Figure 14 shows a comparison of the average temperature of the PCM of the different simulated blocks. As can be seen, concerning the average temperature the segmented blocks performed very similarly; only the large unsegmented block exhibited a different behavior from about 5 hours of melting onwards. The average PCM temperature first was higher than for the other cases (5–9 hours), then lower (9–16 hours) and finally moved towards the same average. This corresponded with more material in the unsegmented block being in the liquid phase during the time from 5 to 9 hours. After about 9–10 hours all material had melted but the bottom part of the unsegmented block still was a bit cooler (larger temperature gradient between top and bottom). After about 16 hours the total amount of heat stored inside the PCM block was, however, similar for each configuration and the temperature converged towards a steady-state condition (Figure 14).

This steady-state condition happens when the mean temperature of the PCM at the surface of the side unexposed to the radiation source had risen to about 50 °C, the heat loss at that side (10 $\text{W/m}^2/\text{K} \cdot (50 \text{ °C} - 20 \text{ °C}) = 300 \text{ W/m}^2$) would become the same as the heat gain from the radiation source on the other side (300 W/m^2). This happened a little before 16 hours of melting. The storage

Energies **2019**, 12, 3286 13 of 16

capacity of the stack of PCM at that point was around 1.8 MJ, which corresponded with the values towards which the total heat stored in the PCM converged (Figure 15).

All the segmented blocks exhibited sensible heat storage during approximately the first 15 to 30 minutes, then latent heat storage with a smaller temperature increase per unit time, for the segmented blocks until about 7 hours, and then again sensible heat storage with a higher temperature increase per unit time (Figure 14). The slope of this last part with sensible heat storage slowly decreased over time because the system converged towards a steady-state condition (see explanation before).

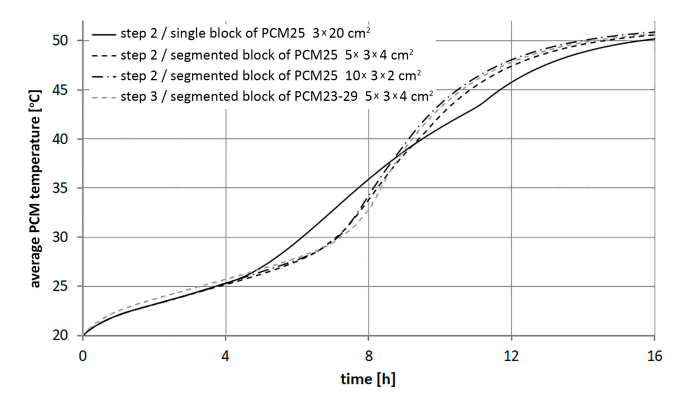


Figure 14. Comparison of the average PCM temperature for four different simulations.

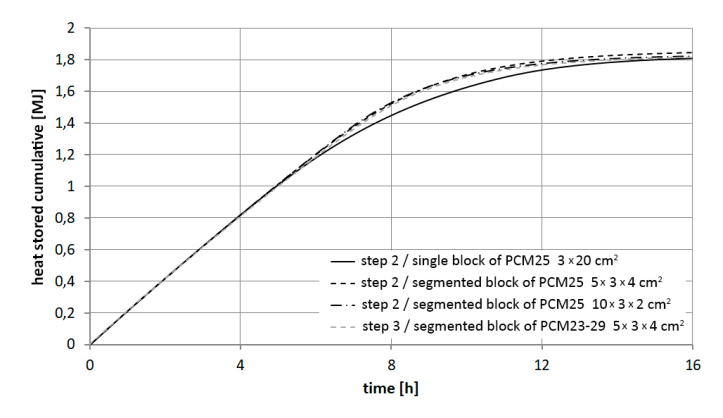


Figure 15. Total amount of accumulated heat stored inside the PCM block.

3.6. Limitations of This Study

In this study a constant inward heat flux of 300 W/m² was applied. For applications in facades of buildings, however, the heat flux was not a constant but varied throughout the day. Furthermore, in that case the heat flux was a short wave solar radiation instead of the long wave radiation as used in this study. That means that for real application the speed of the melting process would be different. However, the basic conclusions still remained valid.

In the present study we also assumed that the boundary around the PCM was opaque for the radiation to which it was exposed. This assumption may or may not be valid for real applications in facades, depending on the encasing used for the PCM. If the encasing is opaque for solar radiation, then that matches well will be the simulation performed in this study. However, if the encasing is transparent for solar radiation, like in case of a glass encasing, the solar radiation will directly penetrate into the PCM. The PCM itself is opaque to solar radiation in solid form but is partially transparent to solar radiation in liquid form. An interesting follow up would be to investigate on a detailed level how solar radiation is being absorbed by the PCM throughout its thickness. That will impact the melting process and may change which solutions for overcoming the heating process are preferred.

Energies 2019, 12, 3286 14 of 16

Finally, in our study we selected a thickness of 3 cm for the column of PCM. Based on preliminary calculations that would be a good thickness for winter conditions in a temperature climate for the total latent heat storage capacity matches with the amount of solar radiation on a sunny winter's day. However, generally manufacturers advise to use thinner layers in the order of 1 to 1.5 cm to make sure that the PCM can cool sufficiently quickly for a daily cycle. Thinner layers will lead to a different behavior because they melt and heat up faster. However, also here the general conclusions from this paper would remain valid.

4. Conclusions

In this paper the melting behavior of phase change material for application in facades of buildings was investigated. It was found that once part of the PCM had melted convection arose in the liquid PCM transporting heat from the bottom of the block to its top. As a result, the top of a block heated up faster than the bottom speeding up the melting process there. This was also reflected by the isotherms that started to curve close to the top. Furthermore, in high columns of PCM a large temperature gradient might arise due to this heat transport phenomenon, especially during the first several hours of the melting process. Since many PCMs have an upper temperature limit, this overheating is a phenomenon that needs careful consideration.

Segmenting a large volume of PCM into smaller volumes (in height direction) ensured that heat was not transferred from the bottom to the top via convection. The convection now only takes place in smaller cells and the respective temperature gradient inside the cell is smaller. This ensures that less heat is transported to the top of the PCM stack as a result of which the bottom segments will start melting faster reducing the temperature gradient between the bottom and the top. The advantage of this is that when using a PCM that is transparent in the melted state in facade applications a more controlled transparency can be obtained. This will be an important requirement for such applications in practice.

Furthermore, the time and uniformity of melting could be controlled as well by stacking PCMs with different melting temperature on top of each other; choosing a lower than average melting temperature at the bottom of the stack will make sure that the bottom will start melting sooner whereas choosing a higher than average melting temperature at the top of the stack will make sure that the top will start melting later. By choosing the right melting temperatures, also the temperature gradient in a column of PCM can be controlled. This solution was found to give the most promising results for minimizing the overheating effect. Selecting the optimal phase change temperatures however is critical. Selecting the wrong temperatures may even aggravate the problem.

Author Contributions: M.T.: funding acquisition, project coordination, conceptualization, methodology, investigation, formal analysis, validation, writing (original draft), writing (review&editing); Y.W.: conceptualization, investigation, formal analysis, validation, writing (review&editing); M.T.: funding acquisition, project coordination, conceptualization, methodology; T.C.: conceptualization; S.T.: conceptualization.

Funding: The Double Face 2.0 project is part of the research program Research through Design with project number 14574, which is financed by the Netherlands Organization for Scientific Research (NWO) and Taskforce for Applied Research SIA.

Acknowledgments: We are also grateful for the help and knowledge provided by the project's partners from industry: Shau Architecture and Urbanism, GlassX AG, Esteco SpA, Rubitherm GmbH and Arup. The researchers would also like to thank MgM Robotics for the technical support and advice when using a Comau robot, which was used for the construction of a prototype for the Architecture Biennale 2018 in Venice.

Conflicts of Interest: The authors declare no conflict of interest. Furthermore, the sponsors had no role in the design, execution, interpretation, or writing of the study; according to procedure, they were however asked if they agreed with publishing this paper; no objections were raised.

References

 Buildings. Available online: https://ec.europa.eu/energy/en/topics/energy-efficiency/buildings (accessed on 24 September 2018). Energies **2019**, 12, 3286 15 of 16

Jeong, S.-G.; Chung, O.; Yu, S.; Kim, S.; Kim, S. Improvement of the thermal properties of Bio-based PCM using exfoliated graphite nanoplatelets. Sol. Energy Mater. Sol. Cells 2013, 117, 87–92.

- 3. Baetens, R.; Jelle, B.P.; Gustavsen, A. Phase change materials for building applications: A state-of-the-art review. *Energy Build.* **2010**, *42*, 1361–1368.
- 4. Kalnaes, S.E.; Jelle, B.P. Phase change materials and products for building applications: A state-of-the-art review and future research opportunities. *Energy Build.* **2015**, *94*, 150–176.
- Patel, J.H.; Darji, P.H.; Qureshi, M.N. Phase change material with thermal energy storage systems and its applications: A systematic review. *Indian J. Sci. Technol.* 2017, 10, 1–10.
- Tyagi, V.V.; Buddhi, D. PCM thermal storage in buildings: A state of art. Renew. Sustain. Energy Rev. 2007, 11, 1146–1166.
- Bland, A.; Khzouz, M.; Statheros, T.; Gkanas, E.I. PCMS for residential building applications: A short review focussed on disadvantages and proposals for future development. *Buildings* 2017, 7, 78.
- Gutherz, J.M.; Schiler, M.E. A passive solar heating system for the perimeter zone of office buildings. *Energy Sources* 1991, 13, 39–54.
- 9. Weinläder, H.; Beck, A.; Fricke, J. PCM-façade-panel for daylighting and room heating. *Sol. Energy* **2005**, 78, 177–186.
- Soares, N.; Samagaio, A.; Vicente, R.; Costa, J. Numerical simulation of a PCM shutter for buildings space heating during the winter. In Proceedings of the 2011 World Renewable Energy Congress, Linköping, Sweden, 8–13 May, 2011; pp. 1797–1804.
- 11. Fiorito, F. Trombe walls for lightweight buildings in temperate and hot climates. Exploring the use of pcms for performance improvement. *Energy Proceedia* **2012**, *30*, 1110–1119.
- 12. Goia, F.; Perino, M.; Serra, V. Improving thermal comfort conditions by means of PCM glazing systems. *Energy Build.* **2013**, *60*, 442–452.
- Goia, F.; Perino, M.; Serra, V. Experimental analysis of the energy performance of a fullscale PCM glazing prototype. Sol. Energy 2014, 100, 217–233.
- 14. Turrin, M.; Tenpierik, M.; de Ruiter, P.; van der Spoel, W.; Chang Lara, C.; Heinzelmann, F.; Teuffel, P.; van Bommel, W. Double Face: Adjustable translucent system to improve thermal comfort. *SPOOL* **2014**, *1*, 5–9. doi:10.7480/spool.2014.2.929.
- Wang, Q.; Zhao, C.Y. Parametric investigations of using PCM curtain for energy efficient buildings. *Energy Build.* 2015, 94, 33–42.
- Wattez, Y.; Cosmatu, T.; Tenpierik, M.; Turrin, M.; Heinzelmann, F. Renewed Trombe wall passively reduces energy consumption. In Proceedings of the 33rd International Conference on Passive and Low Energy Architecture, Edinburgh, UK, 2–5 July 2017; pp. 902–909.
- 17. Tenpierik, M.; Turrin, M.; Wattez, Y.; Cosmatu, T.; Tsafou, S. Double Face 2.0: A lightweight translucent adaptable Trombe wall. *SPOOL* **2018**, *5*, doi:10.7480/spool.2018.2.2090.
- 18. Weinläder, H.; Körner, W.; Heidenfelder, M. Monitoring results of an interior sun protection system with integrated latent heat storage. *Energy Build*. **2011**, *43*, 2468–2475.
- 19. Komerska, A.; Bianco, L.; Serra, V.; Fantucci, S.; Rosinski, M. Experimental analysis of an external dynamic solar shading integrating PCMs: First results. *Energy Proceedia* **2015**, *78*, 3452–3457.
- Li, Y.; Dakwa, J.; Kokgiannakis, G. Experimental evaluation of an integrated phase change material blind system for double skin façade buildings. In Proceedings of the 14th International Conference on Sustainable Energy Technologies, Nottingham, UK, 25–27 August 2015; pp. 1–7.
- 21. Jegadheeswaran, S.; Pohekar, S.D. Performance enhancement in latent heat thermal storage system: A review. *Renew. Sustain. Energy Rev.* **2009**, *13*, 2225–2244.
- 22. Murray, R.E.; Groulx, D. Modeling Convection during Melting of a Phase Change Material. In Proceedings of the 2011 COMSOL Conference, Boston, MA, USA, 13–15 October 2011; pp. 1–7.
- 23. Bertrand, O.; Binet, B.; Combeau, H.; Couturier, S.; Delannoy, Y.; Gobin, D.; Lacroix, M.; Le Quéré, P.; Médale, M.; Mencinger, J.; et al. Melting driven by natural convection. A comparison exercise: First results. *Int. J. Therm. Sci.* **1999**, *38*, 5–26.
- 24. Tay, N.H.S.; Belusko, M.; Liu, M.; Bruno, F. Investigation of the effect of dynamic melting in a tube-in-tank PCM system using a CFD model. *Appl. Energy* **2015**, *137*, 738–747.

Energies **2019**, 12, 3286

25. Ogoh, W.; Groulx, D. Effects of the Heat Transfer Fluid Velocity on the Storage Characteristics of a Cylindrical Latent Heat Energy Storage System: A Numerical Study. *Heat Mass Transf.* **2012**, *48*, 439–449.

26. Castellon, C.; Castell, A.; Medrano, M.; Martorell, M.; Cabeza, L.F. Experimental Study of PCM Inclusion in Different Building Envelopes. *J. Sol. Energy Eng.* **2009**, *131*, 1–6.



© 2019 by the authors. Licensee MDPI, Basel, Switzerland. This article is an open access article distributed under the terms and conditions of the Creative Commons Attribution (CC BY) license (http://creativecommons.org/licenses/by/4.0/).